Article

Use of Pressure in Rotational Molding to Reduce Cycle Times: Comparison of the Thermomechanical Behavior of Rotomolded Reed/Polyethylene Composites

Zaida Ortega [1,*], Luis Suárez [2], Jake Kelly-Walley [3,4], Paul R. Hanna [5], Mark McCourt [5] and Bronagh Millar [5]

1 Departamento de Ingeniería de Procesos, Universidad de Las Palmas de Gran Canaria, Edificio de Ingenierías, Campus Universitario de Tafira Baja, 35017 Las Palmas de Gran Canaria, Spain

2 Departamento de Ingeniería Mecánica, Universidad de Las Palmas de Gran Canaria, Edificio de Ingenierías, Campus Universitario de Tafira Baja, 35017 Las Palmas de Gran Canaria, Spain; luis.suarez@ulpgc.es

3 Matrix Polymers, Unit 2, Compass Industrial Park, Spindus Road, Speke, Liverpool L24 1YA, UK; jake.kelly-walley@matrixpolymers.com

4 Polymer Processing Research Centre, School of Mechanical and Aerospace Engineering, Queen's University Belfast, Ashby Building, Stranmillis Road, Belfast BT9 5AH, UK

5 Polymer Processing Research Centre, Queen's University of Belfast, Ashby Building, Stranmillis Road, Belfast BT9 5AH, UK; p.r.hanna@qub.ac.uk (P.R.H.); m.mccourt@qub.ac.uk (M.M.); b.millar@qub.ac.uk (B.M.)

* Correspondence: zaida.ortega@ulpgc.es

Abstract: Rotational molding advantages include the production of a hollow part with no welding lines, either of small or big sizes, with no internal stresses and good surface details. However, the process is limited by the long cycle times, and its related high energy consumption. Different strategies can be followed to reduce such energy use. This work assesses the use of pressure inside the molds during the densification and cooling stages, finding reductions in overall cycle time of approximately 20%, because of the reduction in the heating time required but also to the increased cooling rate. The influence of such an approach on the production of composites with reed fibers has also been assessed, finding a similar trend towards cycle time reductions. The rotomolded samples' thermomechanical and rheological behavior were determined, finding that viscosity was not affected due to the incorporation of air during the moldings; besides, the homogeneity of the composites increased due to the mold pressurization. The parts obtained show good aesthetics and good thermomechanical behavior along the entire temperature range studied, and particularly for 10% composites; higher fiber ratios should be prepared via melt compounding. Therefore, the mold pressurization allows us to reduce both oven and cooling times, which can be translated into an increase in productivity and a decrease in energy consumption, which are undeniably related to the increase in the products' sustainability and cost.

Keywords: rotomolding; cycle time reduction; pressure; energy consumption; DMA; composite; rheology

1. Introduction

Rotational molding is a well-established manufacturing method that allows obtaining parts with low-cost tooling, no welding lines, no internal stress, and minimal or no waste [1,2]. The use of relatively high temperatures and long cycle times [3], together with the need of having the material either as a powder or as a liquid, limits the materials suited for use within this process, and thus, limit its application [2,4]. In any case, the market share of rotational molding is constantly growing at approximately 6%, and it is expected to reach a value of 8,500 million euros by 2031 [5], by finding new applications, such as hydrogen storage tanks [6] or wind-blade turbines [7,8].

The most common material in rotomolding is polyethylene (PE), in powder form, accounting for about 85% of the market [2], followed by polylactide (PLA) as a more

sustainable alternative [9–11]. The vast use of PE is due to its thermal resistance, low cost, durability, and rheological characteristics [12–14], as the low viscosity of the materials is needed to ensure good sintering of the granules to obtain a well-consolidated part, free of voids and porosity [15].

The process has different stages, which can be simplified into four fundamental ones [12,16]:

1. Introduction of the material inside the mold
2. Rotational molding itself: the mold is introduced into an oven and the rotation starts. During this time, the internal air temperature is usually monitored, observing three stages:
    a. Induction, where the material starts increasing temperature.
    b. Sintering, the powder starts melting and sticking in the mold walls.
    c. Densification: the temperature increases quickly, until reaching the peak internal air temperature (PIAT), which is the maximum temperature reached in the process, and the molten material is consolidated. In this stage, air bubbles trapped in the molten material migrate towards the inside of the part and escape through the mold vent [12–14]
3. Once the desired temperature is reached, the mold is removed from the oven, while still rotating, and the cooling stage starts.
4. Demolding of the part, once the polymer is solidified, the part is extracted from the mold.

In order to overcome rotational molding's limitations and increase its sustainable character, a number of innovations have been incorporated in the sector. These range from the incorporation of bio-based [17–23] or recycled materials [24–28] to the use of innovative tools [29–31].

Previous research works have shown the potential applications of natural fibers or waste materials as fillers of rotomolded parts, as a way to broaden the range of materials available and increase the range of properties achievable while, at the same time, improving the environmental behavior of the molded parts and potentially reducing their costs [12,32]. However, particularly for fillers of an organic nature, the process conditions (namely, relatively high temperature and long cycle time) sometimes make it necessary to treat them in order to increase thermal resistance and avoid degradation. Mercerization (biomass treatment with an NaOH solution) is one of the most commonly applied procedures [32–35], although some authors report the formation of fiber clusters when using this treatment [21,36]; the use of maleated polyethylene or the modification of fibers with maleic anhydride have also been proposed in several works [16,37–40], albeit, with the aim of improving compatibility between the hydrophilic fiber and the hydrophobic matrix. Although these are widely used in the literature for the improvement of the properties of natural fiber composites, their effect in rotomolded products is not as clear as in other production processes, such as injection molding, particularly due to the lack of shear and pressure within the process. Specifically, the use of giant reed fibers (*Arundo donax* L.) has been recently explored in the literature to obtain rotomolded composites; for example, Suárez et al. introduced them in proportions up to 10% in (PLA) and PE matrices, finding a strong correlation between increased fiber loading and porosity, leading to lowered mechanical properties, particularly impact strength and tensile stress [17]. The incorporation of such fibers led to improved biodisintegration behavior for the composites obtained with the PLA matrix; similarly, the research conducted by Ortega and his collaborators [18] reached up to 20% of reed fibers in PE matrices, although with important drops in their mechanical properties. Very few other significant publications have been found on the use of this fibers for composites obtained on rotomolding, while very few additional ones can be retrieved for other processing technologies; for example, Fiore et al. and Suárez et al. have obtained reed composites with PLA, PE, and PP composites, obtaining good

mechanical properties [41,42]. Other authors have obtained composites with this plant using epoxy or polyurethane matrices [43–45].

Concerning energy consumption and its reduction, very little research was found in the literature to the best of the authors' knowledge, and it was mainly related to electrically-heated tools [29] or microwave-assisted processes [31]. The use of directly heated molds, using Robomould device [29], results in a lower energy consumption (by a factor of up to 15 less than in conventional carrousel machines), higher energy efficiency, and a shorter cycle time (about 20%) due to the reduced time needed to heat the mold. A different strategy to reduce the cycle time and improve the final parts' properties (such as reduced shrinkage or increased ductility) is the use of internal pressurization. Only one reference has been found in this sense; Malnati [46] reported cycle time reductions of up to 78% for 6.35 mm thick parts made on PE when using pressure-assisted cooling by Ripple's technology. However, this author only provides the data and neither the curves nor the properties of the obtained parts are reported in that reference.

This paper analyzes the processing cycles to obtain 4 mm thick PE parts when using conventional procedure and two levels of pressure, as well as two different PIATs. The procedure was also applied to obtain composites with lignocellulose fibers, demonstrating the benefits of using such a simple procedure, without the need for complicated modifications in conventional rotomolding machines.

2. Materials and Methods

2.1. Materials

The material used was a polyethylene–hexene grade material produced by Matrix Polymers (Revolve N-307) (Liverpool, UK), with a density of 0.939 g/cm^3 and a melt flow index of 3.5 g/10 min, in powder form. The composites were prepared by dry blending of this PE at a 10 and 20% weight of giant reed fibers, cut to about 2–3 mm in length. These fibers, obtained from *Arundo donax* L. culms by a chemo-mechanical procedure previously described [47], have a cellulose content of over 70% and exhibit good thermal stability.

2.2. Rotational Molding Trials

Samples were produced in a 200 × 200 × 200 mm aluminum mold with a vent hole in a biaxial three-arm carrousel rotomolding machine from Ferry RotoSpeed, the RS–1600 Turret Style model. The rotational speed ratio was set to 8:2, and the oven temperature was set at 300 °C. The oven and peak internal air temperature (PIAT) were constantly monitored using a Rotolog system (Ferry Industries, Stow, OH, USA). For the parts with positive internal pressure applied, the vent was substituted by a pipe with a valve, which was open for the outlet of gases during the first stages of heating and closed for air injection when the sintering stage was concluded.

Samples without pressure application were heated up until reaching an IAT of 180 °C; for those with pressure, the mold was taken out of the oven on reaching 140 °C, at two different pressures: 80 and 150 kPa (0.8 and 1.5 bar). The cooling was performed with forced air until reaching 70 °C, when the parts were extracted from the mold. The total weight of the material in each sample was 800 g, which allowed obtaining 4 mm thick parts. Table 1 summarizes the conditions of the molding trials and the short names given to the obtained parts:

Table 1. Conditions for the different moldings performed.

Short Name	Pressure (kPa)	IAT (°C)	Fiber Content (% Weight)
PE	Ambient	180	0
PE180-0.8	80	180	0
PE140-0.8	80	140	0
PE140-1.5	150	140	0

Table 1. *Cont.*

Short Name	Pressure (kPa)	IAT (°C)	Fiber Content (% Weight)
10A	Ambient	180	10
20A	Ambient	180	20
10A-0.8	80	140	10
20A-0.8	80	140	20

2.3. Materials Characterization

An Olympus BX51 optical microscope (Tokyo, Japan) was used for the observation of the rotomolded samples. The presence of voids and bubbles was assessed in the external and internal sides of the different parts obtained, as well as in their cross section.

The flow properties of the materials were assessed in an oscillatory AR G2 rheometer, from TA instruments (New Castle, DE, USA), with 25 mm diameter parallel plates and a 1.5 mm gap in a nitrogen atmosphere. The experiments were conducted at 190 °C. Preliminary assays were performed under the strain sweep mode in order to ensure that later the experiments were placed in the linear viscoelastic region (LVE). In these tests, the strain was varied between 0.1 and 5%. Frequency sweep tests were performed at a 0.5% strain in the LVE in the 100 to 0.01 Hz range. Finally, flow tests were also performed at the same temperature, between a shear rate of 0.01 and 1 Hz.

The thermomechanical properties of different materials were evaluated by dynamic mechanical thermal analysis (DMTA) using a Tritec 2000 device, from Triton Technology (London, UK), under the single cantilever bending method. A strain of 10 μm was applied at a frequency of 1 Hz between −60 and 100 °C, at a heating rate of 2 °C/min.

From the DMA results, the adhesion factor (A) can be obtained, as described by Kubát et al. [48], and simplified according to [9], in which the authors consider that the behavior of the composite is due to the properties of the matrix, the filler, and the interphase (Equation (1)):

$$A = \frac{1}{1 - x_F} \cdot \frac{\tan\delta_C}{\tan\delta_{PE}} - 1 \tag{1}$$

where x_F is the ratio of the filler in the composite (in volume); and $\tan\delta_C$ and $\tan\delta_{PE}$, the damping factors of the composite and the neat PE, respectively.

The entanglement factor (N) is also proposed as an approximation to the intensity of the interaction between matrix and filler/reinforcement, together with the efficiency factor [49,50]. The entanglement factor is usually calculated at several temperatures to evaluate the potential differences in such interactions due to different service conditions; this factor is calculated as

$$N = \frac{E'}{RT} \tag{2}$$

where E' is the storage modulus at a certain temperature (T, in K) and R is the universal gas constant.

The reinforcement efficiency (r), calculated as shown in Equation (3), provides information about the filler/matrix interaction:

$$E'_c = E'_m \cdot (1 + r \cdot V_f) \tag{3}$$

where E'_c and E'_m are the storage moduli of the composite and the matrix, respectively, and V_f is the percentage of the filler (by volume).

3. Results and Discussion

3.1. Cycle Time Analysis

Figure 1 shows the cycles recorded for the PE rotomolding trials; as also found in Table 1, the curves for the moldings at lowest temperature are overlapped regardless of the value of the pressure applied. Apart from this, reductions in oven time are observed,

ranging from 7 to 14% in oven are observed from Figure 1a, while in Figure 1b the shortest overall cycle is clear, together with the increase in the densification rate for all moldings performed under pressure.
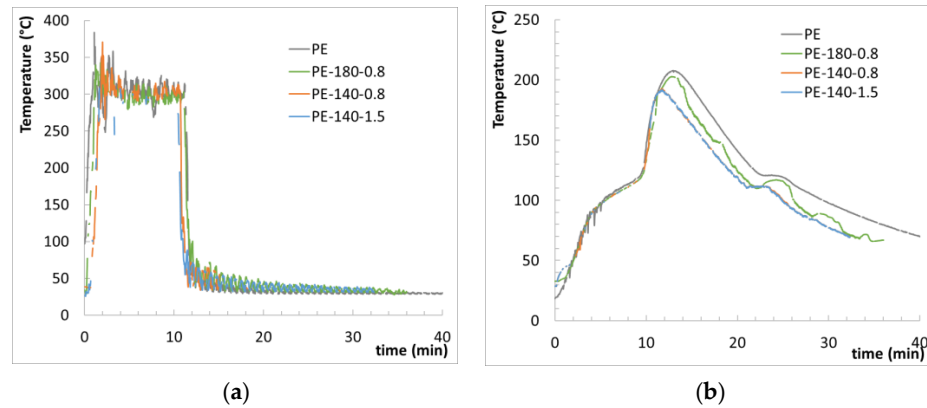
Figure 1. (**a**) Temperature recordings for thermocouple placed outside the mold. (**b**) Monitoring of internal air temperature for PE moldings.

Furthermore, when taking the mold out of the oven at 140 °C, a PIAT of approximately 190 °C is reached, meaning that the pressure on the molten materials force it towards the mold walls and enhance the energy transfer between the mold and the molten material (the moldings with no pressure are taken out of the oven for an IAT of 180 °C, and reach a PIAT of 206.4 °C, that is, an increase of only about 20 °C vs. the approximately 50 °C increase obtained for pressurized moldings). This lower temperature will beneficially result in a reduced extent of degradation, which is of particular interest for polymers (or fillers) sensitive to thermo-oxidation, while, at the same time, it allows getting well-cooked parts and does not negatively affect their properties.

Considering the moldings performed at different values of pressure and the lack of differences observed, the composites were obtained at 80 kPa. A lignocellulosic fiber (from giant reed) was introduced in the PE matrix in order to determine whether the cycle times for composites are also affected by mold pressurization, as previous research work has shown that cycle time is increased by approximately 6% for 10% abaca composites [21]. In Figure 2, it is observed that the composites with reeds tend to delay different stages in the process, particularly the induction step, due to the thermal insulating behavior of the lignocellulose materials, and up to 18% for 20% loaded composites. The use of pressure in this case also results in a decrease in oven time of 10% compared to the same material without pressurization, due to the faster densification step, while a more significant 17% total reduction in cycle time is found due to a faster cooling. More significant differences are observed for 20% composites, as observed in Figure 2:
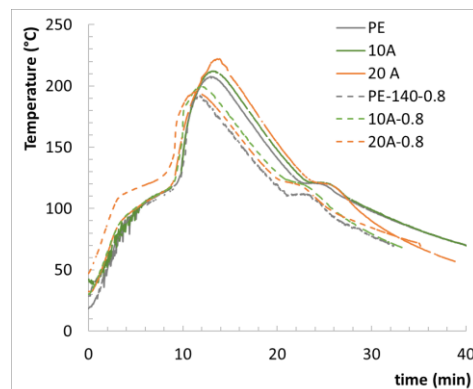

Figure 2. Internal air temperature curves for composites at 10 and 20% loading.

It is then clear that the use of pressurization can effectively reduce the cycle time either of neat PE or composites. Table 2 summarizes the reductions in heating, cooling, and total process cycles for the different moldings; the use of positive pressure effectively decreases the cycle time by approximately 20%, even for composite moldings, with oven time reductions also significant. There is no difference in the cycles due to the use of 80 or 150 kPa; therefore, the first pressure level is enough to achieve the desired shortening of the process. The effectiveness of pressure in cycle reduction is mainly due to the shortening in the cooling stage. In terms of cycle time reduction, linked to energy consumption and productivity, it is particularly interesting to incorporate pressure when working with composites, because this is when the most important cycle time reduction happens, finding a cycle similar to that of neat PE under pressure.

Table 2. Distribution of time for each stage of the rotomolding cycle and variations compared to PE molding cycle without any pressure applied.

Cycle	Oven Time		Cooling Time		Total Cycle Time		PIAT	Time to Reach PIAT	
	(min)	Variation (%)	(min)	Variation (%)	(min)	Variation (%)	(°C)	(min)	Variation (%)
PE	11.9	--	27.3	--	40.3	--	206.4	12.3	--
PE180-0.8	11.0	−7.3	20.2	−25.9	32.0	−20.7	202.3	11.8	−4.5
PE140-0.8	10.6	−11.2	20.7	−24.0	32.3	−19.9	190.2	11.5	−6.2
PE140-1.5	10.4	−12.4	20.6	−24.0	32.2	−19.9	190.6	11.6	−6.2
10A	11.6	−2.9	27.2	−0.4	39.7	−1.6	211.8	12.5	1.4
20A	12.8	7.6	12.2	−22.4	35.2	−12.7	220.7	13.9	12.7
10A-0.8	10.8	−9.2	21.0	−23.1	32.7	−18.8	199.3	11.8	−4.6
20A-0.8	12.0	0.8	18.9	−30.7	32.3	−19.9	198.0	11.2	−9.2

Finally, the molded parts show good consistency, with few voids/bubbles and good fiber distribution in general (Figure 3a,b); besides, the moldings performed with pressure also show less warpage (Figure 3c,d). Due to the shorter cycles, and the lower PIAT, the degradation of the filler is reduced, as clearly observed for the composites with the reed fibers, which exhibit a lighter color for the pressurized moldings.


(a)

(b)

(c)

(d)
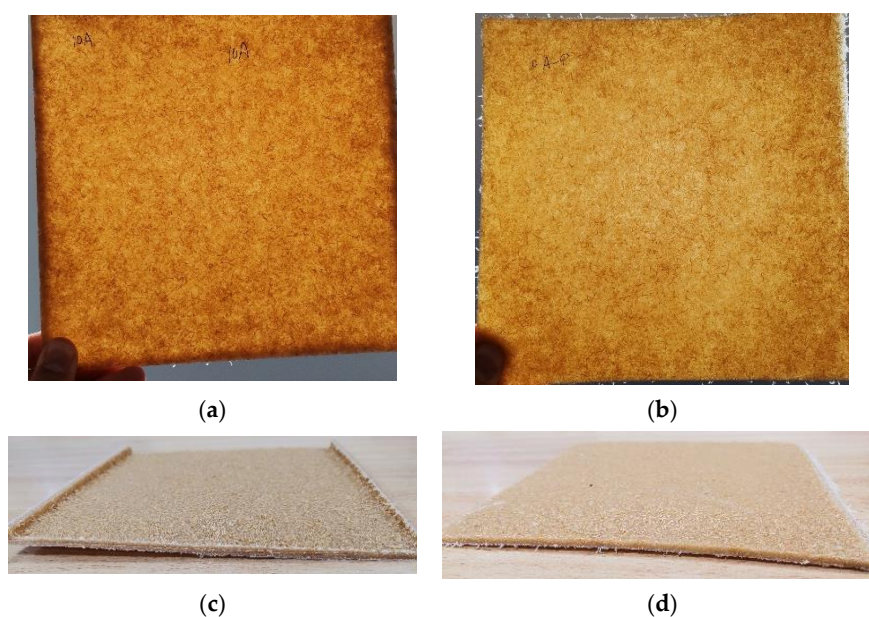
Figure 3. Photographs of 10% composites showing the distribution of fibers for (**a**) 10% fiber, (**b**) 10% fiber under pressure, and the aspect of a side of the cube for (**c**) 10% fiber, (**d**) 10% fiber under pressure.

The observation of samples under optical microscopy allows confirming the fewer bubbles in the polyethylene samples when working under pressure, despite the lower temperature reached (Figure 4). Not only is the internal surface more homogeneous but also the presence of bubbles within the wall thickness is reduced to obtain parts with practically the absence of bubbles. As expected, the incorporation of fibers results in a higher number of defects due to the lack of the shear stress of the process. However, the use of pressure has also been seen to be beneficial for composite production, where a better integration of the fibers within the matrix is observed, as also confirmed later in this document. The most significant differences are found particularly on the inner side of the parts, where the fibers in the pressurized moldings are covered with the polymer, while for moldings without pressure they are looser. In any case, the composites with a 20% fiber content exhibit a high porosity, albeit, again to a lesser extent with the use of pressure.

3.2. Rheology Assessment of Rotomolded Samples

The previous analysis of the storage and loss modulus (G' and G'') versus strain, obtained during strain sweep assays, was performed to ensure that the analysis took place in the linear viscoelastic region (0.1–5.0% strain), selecting the 0.5% strain for the frequency sweep tests. As observed in Figure 5, and suggested in Section 3.1, no differences in the rheological behavior of the PE are observed as a consequence of the incorporation of air pressure during molding in the entire range of frequencies studied. This constitutes proof that no modifications in the bulk material occur in the process regardless of the application of pressure.

The zero-shear viscosity values (η_0) show similar behavior for each material, regardless of the use of pressure, i.e., approximately 2100 Pa·s for PE and 2300 Pa·s for reed composites; therefore, it can be concluded that the fibers do not significantly affect the η_0. Some differences are found for the fibrous composites, particularly in the storage modulus (Figure 6a), where the samples rotomolded without pressure seem to stiffen the matrix to a greater extent, particularly at low frequencies. The reduction in G' found for pressurized moldings, which show a behavior quite close to that for the neat matrix, can be an indication of a better dispersion of the fibers within the parts' thickness, which otherwise tend to move towards the inner surface of the part. This can be confirmed by drawing the Cole-Cole plot (Figure 6b), which is a comparison between the real and imaginary parts of viscosity. The closer the shape obtained to a circle the higher the homogeneity of the blend [51,52]. It can be observed that the curves for fibrous composites show dissimilar behavior, getting a closer approximation to the semicircle for the moldings under pressure; and the fibrous composite without pressurization tend to form a straight line at higher viscosities, indicating that the fibers tend to get agglomerated [51,52]. Finally, Figure 6c shows the complex viscosity for the different molded samples; a Newtonian plateau is observed for all samples, although with some deviations for the composites, particularly at low shear rates, thus meaning that they exhibit a shear thinning behavior. Once more, the more dissimilar behavior is obtained for the fibrous composites without pressure, because of the formation of agglomerates [9].
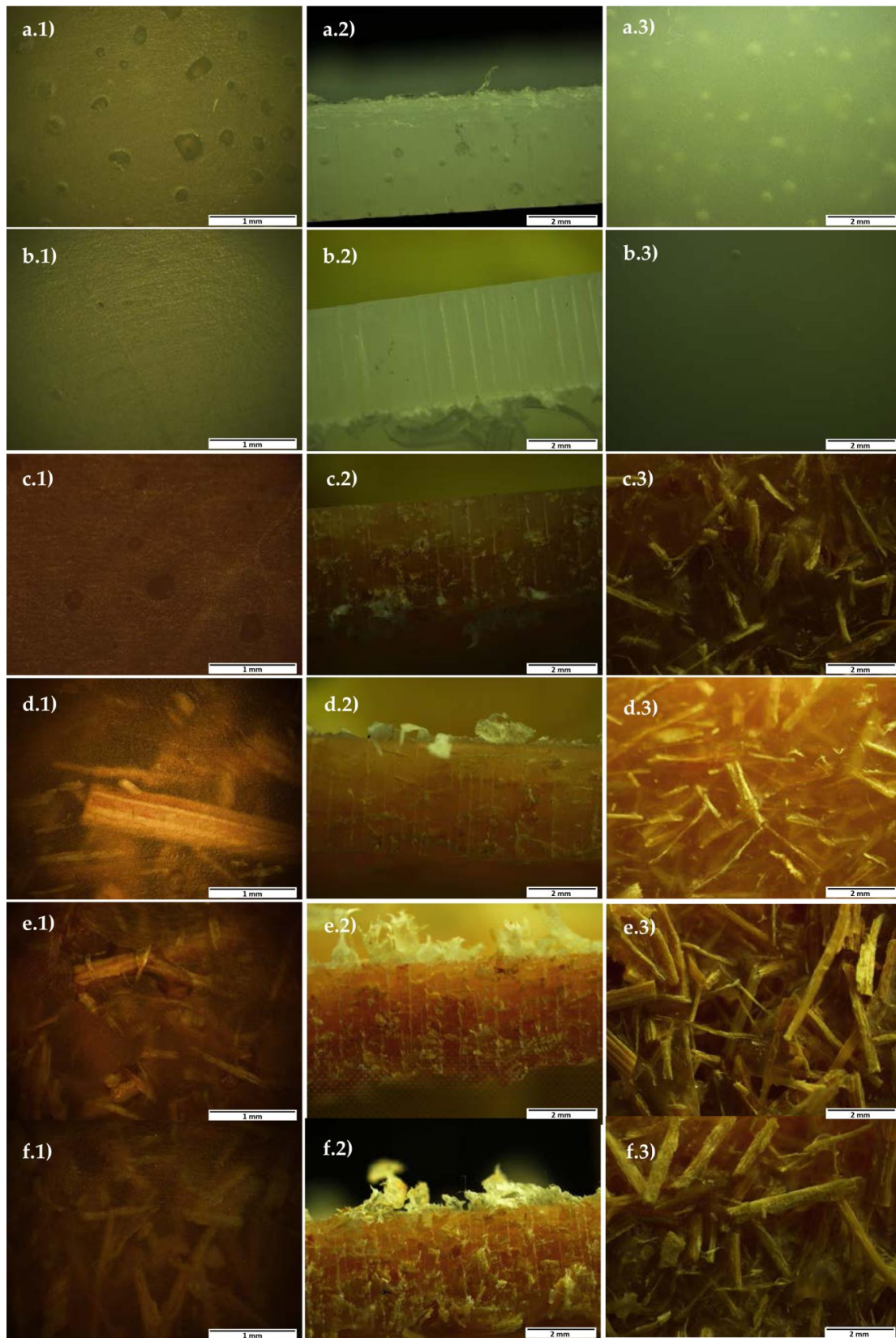
Figure 4. Microscopical observations of (**a**) PE, (**b**) PE-140-0.8, (**c**) 10A, (**d**) 10A-P, (**e**) 20-A, (**f**) 20A-P. Pictures were taken on the external side of the samples (labelled as 1), on the cross section (labelled as 2) and on the internal side (labelled as 3).

(a)   (b)
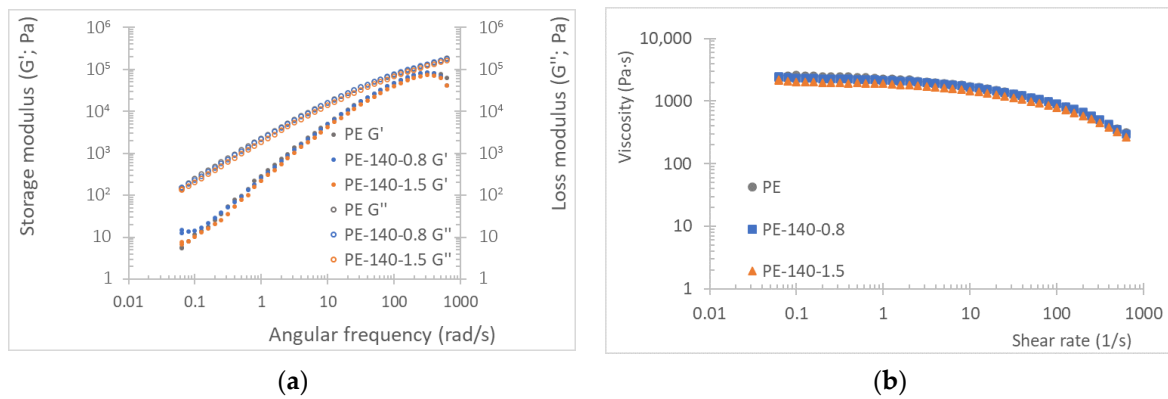
Figure 5. Rheological behavior of PE rotomolded samples: (**a**) storage (left) and loss (right) modulus versus angular frequency, (**b**) viscosity versus shear rate.

(a)   (b)

(c)
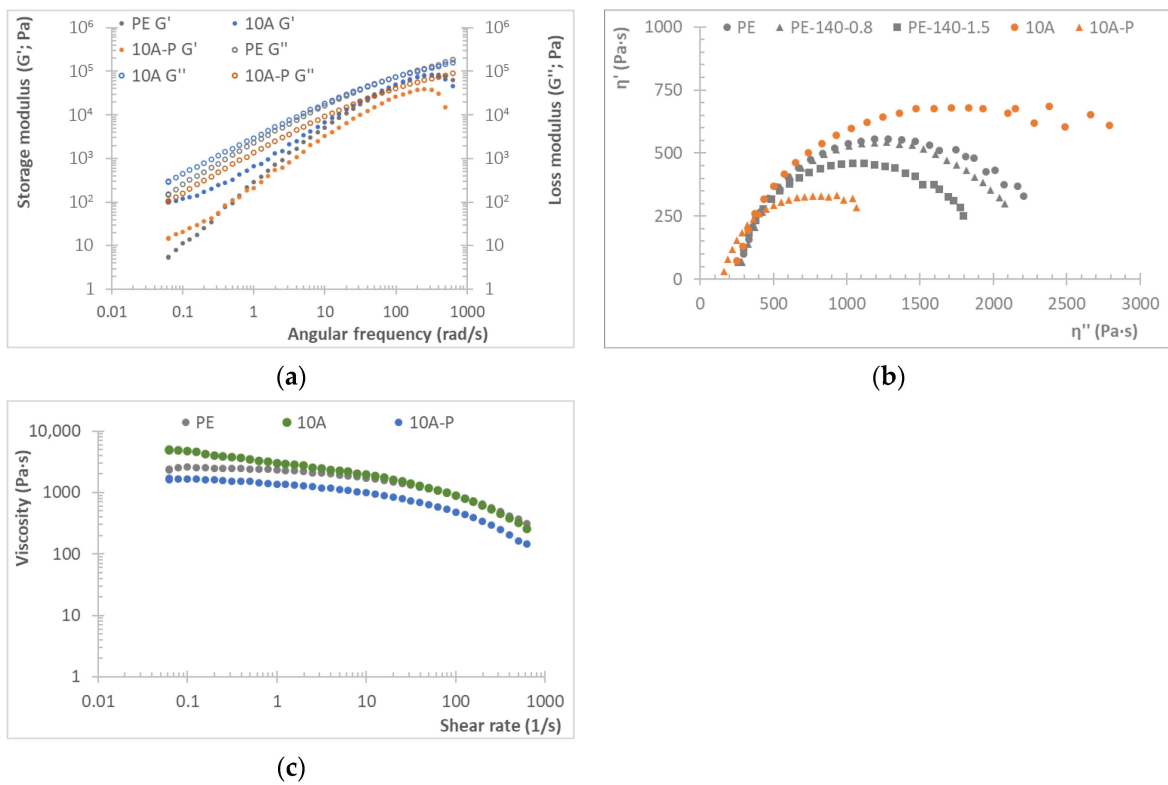
Figure 6. Rheological behavior of the rotomolded samples: (**a**) storage (left) and loss (right) modulus for composites with reed fibers, (**b**) Cole-Cole plot, (**c**) viscosity curves.

3.3. Thermomechanical Performance of Rotomolded Samples

Dynamic mechanical analysis (DMA) is an important test for the evaluation of the mechanical properties of materials because it is sensitive to structural changes [53]. The analysis of the storage modulus (E′), loss modulus (E″), and damping factor (tanδ) with temperature allows for an evaluation of the change in mechanical properties in the temperature range studied (−60 to 100 °C) due to the different processing of the material, namely, the use of pressure and a lower PIAT. The curves for the different moldings of neat PE (Figure 7) follow the expected trend for the storage modulus, with a decreasing trend with temperature. Again, no significant differences are observed for the rotomolded polyethylene samples due to the use of pressure during the moldings. However, the samples rotomolded at higher pressure seem to provid higher values of the storage modulus, that is, a more elastic behavior. For the loss modulus (Figure 7b), the curves overlap,

with two maximums in the curves, one at approximately −20 °C, which can be related to segmental motions in the amorphous region [54], and a more intense one at 44–47 °C, attributed to the α-transition (chain movements in the crystalline region) [9]. These same conclusions arise from the damping factor curves shown in Figure 7a.
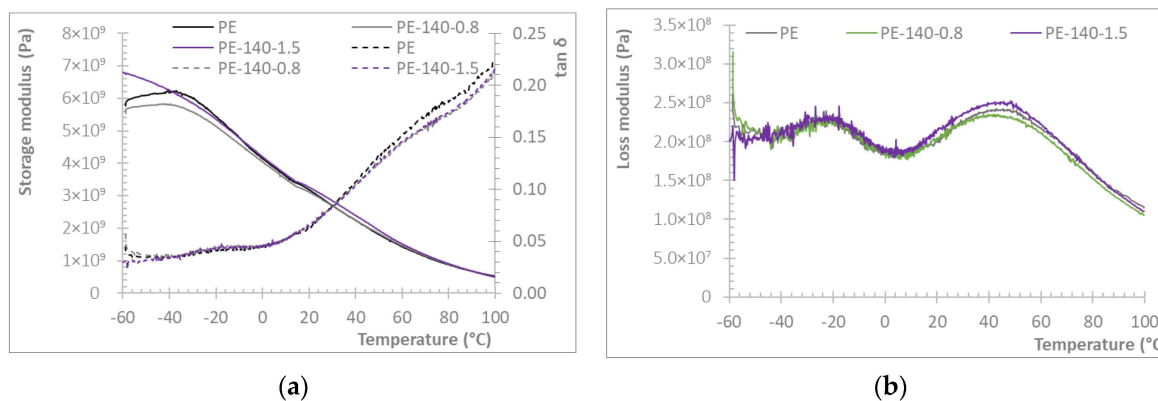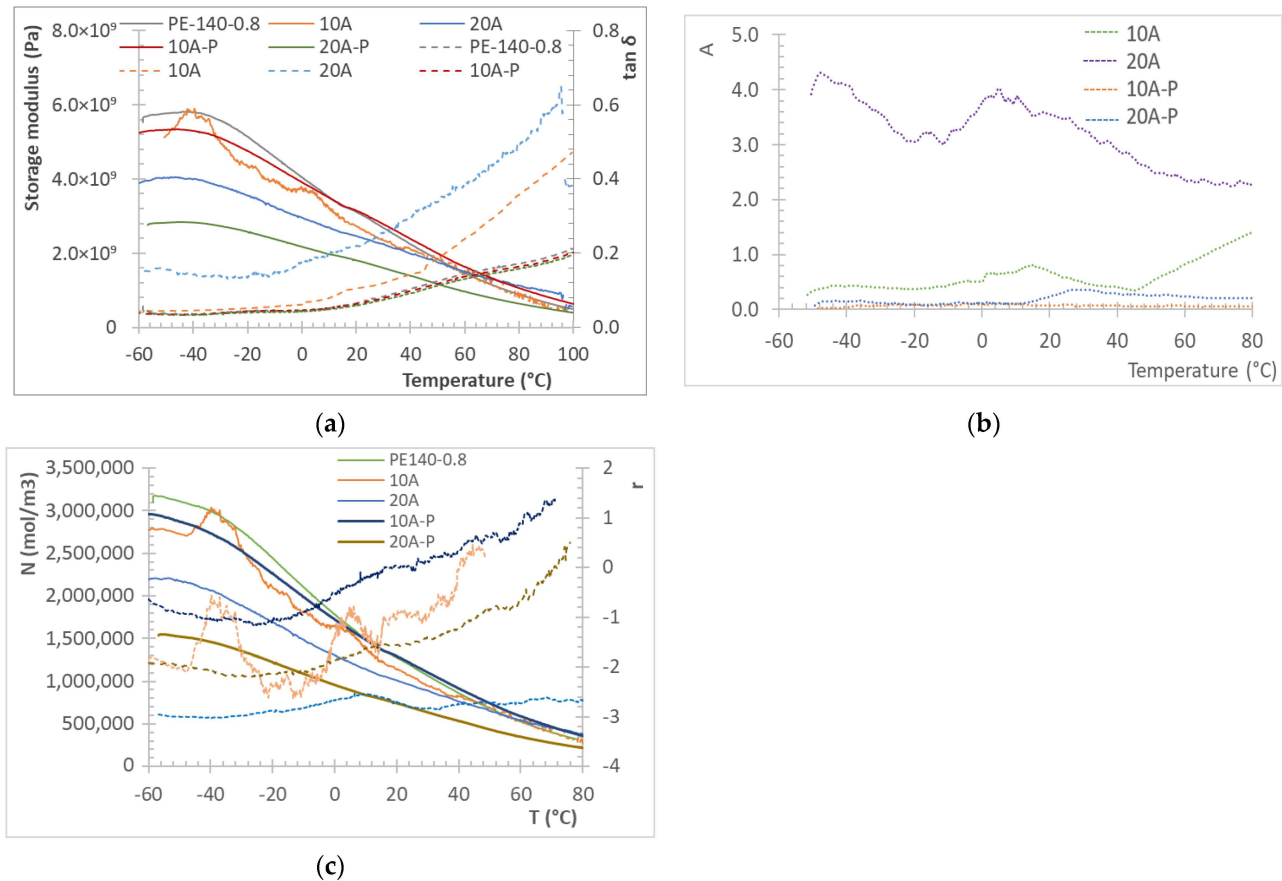

Figure 7. Variation of (**a**) storage modulus and damping factor and (**b**) loss modulus for neat PE rotomolded parts.

When assessing the effect of pressure in the composites, it can be observed that the fibers are not acting as the reinforcement of the matrix, as the storage modulus (responsible for the elastic behavior of the composite) does not increase. However, it can be considered that they are not reducing the mechanical properties of composites significantly when used at 10%, as otherwise expected. It is interesting to note that the fiber length directly affects the mechanical properties of the obtained parts, as well as the interface between the fiber and matrix, and usually the longer the fibers the better the properties [52]. However, it is well known that the particle size distribution affects the properties of rotomolded products to a significant extent [3,18,37], and so a compromise between these two aspects should be achieved. Therefore, this work was performed with relatively short fibers (2–3 mm long, the usual size in any case in rotational molding); longer fibers result in entanglements and poor distribution on the matrix, with reduced mechanical behavior. In any case, it is interesting to note that the use of pressure results in a more stable behavior of the rotomolded part for composites at 10%, as the curve obtained is smoother and closer to that of the PE, even observing a slight increase in the value of the storage modulus for temperatures over 20 °C (Figure 8a). Despite the negative influence of adding 20% of fibers in the values for the storage modulus, it can also be seen that these composites show less variation in the range of temperatures studied; i.e., the properties are less variable with temperature; for this material, the values of storage modulus tend to approximate the ones showed by the matrix from approximately 40 °C. As observed in the moldings, 20% loading overcomes the limit of foreign material use in rotomolding, particularly as compounding was not performed here; this is mainly due to the formation of fiber clusters that hinder the movement of the PE during the process and result in the appearance of voids. For such high loadings, there are no benefits from the use of pressure, at least for this format of filler, with a relatively high aspect ratio.

From Equations (1)–(3) and the DMA results, different factors to assess the adhesion between the fibers and the matrix can be calculated. They are represented in Figure 8b (adhesion factor, A) and Figure 8c (entanglement and reinforcement efficiency, N and r, respectively). The lower values of A indicate a higher interfacial adhesion [9,21], which should result in improved mechanical performance. It can be observed that the samples obtained under pressure provide a lower value of this factor, and also more stable behavior in the temperature range studied. When 20% fiber composites are used, the highest values are attained for A, which are reduced to values even lower than those obtained for 10% composites obtained without pressurization. Moreover, samples 10A-P show an adhesion

factor close to zero in the entire analyzed range, thus demonstrating the potential of pressure application in rotomolded composites, as also determined from the flow behavior. Similarly, the entanglement factor is reduced for all composites, with reinforcement efficiencies under zero, meaning that the fibers are not acting as reinforcement but are reducing the mechanical performance of composites, particularly with a ratio of 20%. However, an improvement in these parameters is also observed for the samples obtained with pressure. Therefore, the application of pressure during the rotational molding of composites can effectively improve the adhesion between the fiber and the matrix, with the advantage of also reducing the processing cycle times.

(a)

(b)

(c)

Figure 8. (**a**) Variation of storage modulus and damping factor for composites with reed fibers, (**b**) adhesion factor (A) evolution with temperature, and (**c**) entanglement factor (N) and reinforcement efficiency (r).

4. Conclusions

The use of positive pressure inside the mold during rotational molding effectively allows for significant reductions of cycle time, thus making the process more efficient in terms of energy consumption. The pressurization of the molds allows us to reduce both oven and cooling times, which can be translated into an increase in productivity and a decrease in energy consumption. Average values of a 20% reduction in cycle time can be achieved by the use of this strategy.

The characterization performed over rotomolded samples allows ensuring that there is no degradation of the polymer due to the incorporation of air within the process; however, in the case of working with polymers more sensitive to thermo-oxidation than polyethylene, the gas could be switched to an inert one, such as nitrogen, thus preventing this effect. The reduction in the peak internal temperature did not lead to a modification of the thermomechanical behavior of the polymer, thus demonstrating that this reduction in

temperature is feasible, while maintaining the mechanical properties and aesthetics of the obtained parts.

Finally, the incorporation of different kinds of fillers can also benefit from the use of pressure during the moldings, also resulting in lower cycle times, and not affecting the mechanical behavior of the rotomolded products. In fact, the rheological behavior seems to be improved as a consequence of the mold pressurization for fibrous composites, obtaining a more homogenous material because of the better dispersion of the fibers; no differences in the thermomechanical behavior of composites due to the use of pressure was found, although composites at 10% fiber loading obtained under mold pressurization exhibit behavior close to that of the neat PE, with even slight improvements of the storage modulus at a temperature above room temperature. The composites with 20% loading resulted in a reduction of their properties, although providing a more stable storage modulus in the studied temperature range; i.e., there are fewer variations of the elastic properties of the material. This amount of fiber is excessive for rotomolding, at least to be obtained only by dry-blending, although well-consolidated parts were obtained.

In summary, the use of pressure during the densification and cooling stages allows for a reduction in the total cycle time of approximately 20%, with the oven time being reduced by about 10%, leading to well-consolidated parts, with no voids or apparent defects, and with a good thermomechanical and rheological behavior for 10% composites. The economic and environmental benefits of such an approach, which does not require extensive modifications in conventional machines or tooling, are then clear. However, some more studies would be needed to determine the effect of such an approach on energy (and costs) savings, particularly when it comes to the production of large parts.

Author Contributions: Conceptualization, Z.O.; methodology, J.K.-W., M.M., P.R.H., L.S. and Z.O.; formal analysis, B.M. and Z.O.; investigation, Z.O., L.S. and P.R.H.; writing—original draft preparation, Z.O.; writing—review and editing, all authors; visualization, L.S.; supervision, Z.O. and M.M. All authors have read and agreed to the published version of the manuscript.

Data Availability Statement: Data will be made available upon reasonable request by the corresponding author.

Conflicts of Interest: Jake Kelly-Walley was employed by the company Matrix Polymers, the remaining authors declare that the research was conducted in the absence of any commercial or financial relationships that could be construed as a potential conflict of interest. The funders had no role in the design of the study; in the collection, analyses, or interpretation of data; in the writing of the manuscript; or in the decision to publish the results.

References

1. Gogos, C.; Tadmor, Z. *Principles of Polymer Processing*, 1st ed.; John Wiley & Sons, Inc.: Toronto, ON, Canada, 1979; Volume 1.
2. Crawford, R.J. *Kearns, M.P. Practical Guide to Rotational Moulding*, 3rd ed.; Elsevier: Amsterdam, The Netherlands, 2020; ISBN 9780128224069.
3. Cramez, M.C.; Oliveira, M.J.; Crawford, R.J. Optimization of the Rotational Moulding Process for Polyolefins. *Proc. Inst. Mech. Eng. B J. Eng. Manuf.* **2003**, *217*, 323–334. [CrossRef]
4. Billmeyer, F. *Textbook of Polymer Science*, 3rd ed.; John Wiley & Sons, Inc.: New York, NY, USA, 1984.
5. Rotomolding Market | Global Industry Report 2023. Available online: https://www.transparencymarketresearch.com/rotomolding-market.html (accessed on 5 December 2022).
6. Shirinbayan, M.; Montazeri, A.; Nouri Sedeh, M.; Abbasnezhad, N.; Fitoussi, J.; Tcharkhrtchi, A. Rotational Molding of Polyamide-12 Nanocomposites: Modeling of the Viscoelastic Behavior. *Int. J. Mater. Form.* **2021**, *14*, 143–152. [CrossRef]

7. Lucas, A.; Danlos, A.; Shirinbayan, M.; Motaharinejad, V.; Paridaens, R.; Benfriha, K.; Bakir, F.; Tcharkhtchi, A. Conventional Rotational Molding Process and Aerodynamic Characteristics of an Axial-Flow Hollow Blades Rotor. *Int. J. Adv. Manuf. Technol.* **2019**, *104*, 1183–1194. [CrossRef]

8. Pereira, M.; Zirak, N.; Shirinbayan, M.; Zywica, G.; Tcharkhtchi, A. Design, Fabrication, and Evaluation of a Small Turbine Blade Manufactured by Rotational Molding. *Int. J. Adv. Manuf. Technol.* **2023**, *128*, 3441–3450. [CrossRef]

9. Hejna, A.; Barczewski, M.; Andrzejewski, J.; Kosmela, P.; Piasecki, A.; Szostak, M.; Kuang, T. Rotational Molding of Linear Low-Density Polyethylene Composites Filled with Wheat Bran. *Polymer* **2020**, *12*, 1004. [CrossRef]

10. Greco, A.; Ferrari, F.; Maffezzoli, A. Processing of Super tough Plasticized PLA by Rotational Molding. *Adv. Polym. Technol.* **2019**, *2019*, 3835829. [CrossRef]

11. Greco, A.; Maffezzoli, A. Rotational Molding of Biodegradable Composites Obtained with PLA Reinforced by the Wooden Backbone of Opuntia Ficus Indica Cladodes. *J. Appl. Polym. Sci.* **2015**, *132*, 42447. [CrossRef]

12. Ogila, K.O.; Shao, M.; Yang, W.; Tan, J. Rotational Molding: A Review of the Models and Materials. *Express Polym. Lett.* **2017**, *11*, 778–798. [CrossRef]

13. Chaudhary, B.I.; Takács, E.; Vlachopoulos, J. Processing Enhancers for Rotational Molding of Polyethylene. *Polym. Eng. Sci.* **2001**, *41*, 1731–1742. [CrossRef]

14. Bellehumeur, C.T.; Bisaria, M.K.; Vlachopoulos, J. An Experimental Study and Model Assessment of Polymer Sintering. *Polym. Eng. Sci.* **1996**, *36*, 2198–2207. [CrossRef]

15. Greco, A.; Maffezzoli, A.; Forleo, S. Rotational Molding of Bio-Polymers. In Proceedings of the PPS-29—AIP Conference Proceedings; American Institute of Physics: College Park, MD, USA, 2014; Volume 1593, pp. 333–337.

16. Hanana, F.E.; Chimeni, D.Y.; Rodrigue, D. Morphology and Mechanical Properties of Maple Reinforced LLDPE Produced by Rotational Moulding: Effect of Fibre Content and Surface Treatment. *Polym. Polym. Compos.* **2018**, *26*, 299–308. [CrossRef]

17. Suárez, L.; Ortega, Z.; Romero, F.; Paz, R.; Marrero, M.D. Influence of Giant Reed Fibers on Mechanical, Thermal, and Disintegration Behavior of Rotomolded PLA and PE Composites. *J. Polym. Env.* **2022**, *30*, 4848–4862. [CrossRef]

18. Ortega, Z.; Romero, F.; Paz, R.; Suárez, L.; Benítez, A.N.; Marrero, M.D. Valorization of Invasive Plants from Macaronesia as Filler Materials in the Production of Natural Fiber Composites by Rotational Molding. *Polymer* **2021**, *13*, 2220. [CrossRef] [PubMed]

19. Cisneros-López, E.O.; Pérez-Fonseca, A.A.; González-García, Y.; Ramírez-Arreola, D.E.; González-Núñez, R.; Rodrigue, D.; Robledo-Ortíz, J.R. Polylactic Acid-Agave Fiber Biocomposites Produced by Rotational Molding: A Comparative Study with Compression Molding. *Adv. Polym. Technol.* **2018**, *37*, 2528–2540. [CrossRef]

20. Andrzejewski, J.; Krawczak, A.; Wesoły, K.; Szostak, M. Rotational Molding of Biocomposites with Addition of Buckwheat Husk Filler. Structure-Property Correlation Assessment for Materials Based on Polyethylene (PE) and Poly(Lactic Acid) PLA. *Compos. B Eng.* **2020**, *202*, 108410. [CrossRef]

21. Ortega, Z.; Suárez, L.; Kelly-Walley, J.; McCourt, M. Mechanical Properties of Rotomolded Parts with Abaca Fiber: Effect of Manufacturing with 1, 2 or 3 Layers. *Compos. Theory Pract.* **2023**, *3*, 158–166.

22. Aniśko, J.; Barczewski, M. Uniaxial Rotational Molding of Bio-Based Low-Density Polyethylene Filled with Black Tea Waste. *Materials* **2023**, *16*, 3641. [CrossRef]

23. Szostak, M.; Tomaszewska, N.; Kozlowski, R. Mechanical and Thermal Properties of Rotational Molded PE/Flax and PE/Hemp Composites. *Lect. Notes Mech. Eng.* **2019**, 495–506. [CrossRef]

24. Cestari, S.P.; Martin, P.J.; Hanna, P.R.; Kearns, M.P.; Mendes, L.C.; Millar, B. Use of Virgin/Recycled Polyethylene Blends in Rotational Moulding. *J. Polym. Eng.* **2021**, *41*, 509–516. [CrossRef]

25. Pick, L.; Hanna, P.R.; Gorman, L. Assessment of Processibility and Properties of Raw Post-Consumer Waste Polyethylene in the Rotational Moulding Process. *J. Polym. Eng.* **2022**, *42*, 374–383. [CrossRef]

26. Aniśko, J.; Barczewski, M.; Mietliński, P.; Piasecki, A.; Szulc, J. Valorization of Disposable Polylactide (PLA) Cups by Rotational Molding Technology: The Influence of Pre-Processing Grinding and Thermal Treatment. *Polym. Test.* **2022**, *107*, 107481. [CrossRef]

27. Arribasplata-Seguin, A.; Quispe-Dominguez, R.; Tupia-Anticona, W.; Acosta-Sullcahuamán, J. Rotational Molding Parameters of Wood-Plastic Composite Materials Made of Recycled High Density Polyethylene and Wood Particles. *Compos. B Eng.* **2021**, *217*, 108876. [CrossRef]

28. Dou, Y.; Rodrigue, D. Morphological, Thermal and Mechanical Properties of Recycled HDPE Foams via Rotational Molding. *J. Cell. Plast.* **2022**, *58*, 305–323. [CrossRef]

29. McCourt, M.; Kearns, M.P.; Martin, P.; Butterfield, J. A Comparison between Conventional and Robotic Rotational Moulding Machines. In Proceedings of the IMC34—34th International Manufacturing Conference At: Sligo Institute of Technology, Sligo, Ireland, 30–31 August 2017.

30. Ortega, F.; Sova, A.; Monzón, M.D.; Marrero, M.D.; Benítez, A.N.; Bertrand, P. Combination of Electroforming and Cold Gas Dynamic Spray for Fabrication of Rotational Moulds: Feasibility Study. *Int. J. Adv. Manuf. Technol.* **2015**, *76*, 1243–1251. [CrossRef]

31. Luciano, G.; Vignolo, M.; Brunengo, E.; Utzeri, R.; Stagnaro, P. Study of Microwave-Active Composite Materials to Improve the Polyethylene Rotomolding Process. *Polymer* **2023**, *15*, 1061. [CrossRef] [PubMed]

32. León, L.D.V.E.; Escocio, V.A.; Visconte, L.L.Y.; Junior, J.C.J.; Pacheco, E.B.A.V. Rotomolding and Polyethylene Composites with Rotomolded Lignocellulosic Materials: A Review. *J. Reinf. Plast. Compos.* **2020**, *39*, 459–472. [CrossRef]

33. Torres, F.G.; Aragon, C.L. Final Product Testing of Rotational Moulded Natural Fibre-Reinforced Polyethylene. *Polym. Test.* **2006**, *25*, 568–577. [CrossRef]

34. Wang, B.; Panigrahi, S.; Tabil, L.; Crerar, W. Pre-Treatment of Flax Fibers for Use in Rotationally Molded Biocomposites. *J. Reinf. Plast. Compos.* **2007**, *26*, 447–463. [CrossRef]

35. Oliveira, M.A.S.; Pickering, K.L.; Sunny, T.; Lin, R.J.T. Treatment of Hemp Fibres for Use in Rotational Moulding. *J. Polym. Res.* **2021**, *28*, 53. [CrossRef]

36. Ortega, Z.; Monzón, M.D.; Benítez, A.N.; Kearns, M.; McCourt, M.; Hornsby, P.R. Banana and Abaca Fiber-Reinforced Plastic Composites Obtained by Rotational Molding Process. *Mater. Manuf. Process.* **2013**, *28*, 130614085148001. [CrossRef]

37. Hanana, F.E.; Rodrigue, D. Effect of Particle Size, Fiber Content, and Surface Treatment on the Mechanical Properties of Maple-Reinforced LLDPE Produced by Rotational Molding. *Polym. Polym. Compos.* **2021**, *29*, 343–353. [CrossRef]

38. Hanana, F.E.; Rodrigue, D. Rotational Molding of Polymer Composites Reinforced with Natural Fibers. *Plast. Eng.* **2015**, *71*, 28–31. [CrossRef]

39. Hanana, F.E.; Rodrigue, D. Rotational Molding of Self-Hybrid Composites Based on Linear Low-Density Polyethylene and Maple Fibers. *Polym. Compos.* **2018**, *39*, 4094–4103. [CrossRef]

40. Cisneros-López, E.O.; González-López, M.E.; Pérez-Fonseca, A.A.; González-Núñez, R.; Rodrigue, D.; Robledo-Ortíz, J.R. Effect of Fiber Content and Surface Treatment on the Mechanical Properties of Natural Fiber Composites Produced by Rotomolding. *Compos. Interfaces* **2017**, *24*, 35–53. [CrossRef]

41. Fiore, V.; Botta, L.; Scaffaro, R.; Valenza, A.; Pirrotta, A. PLA Based Biocomposites Reinforced with Arundo Donax Fillers. *Compos. Sci. Technol.* **2014**, *105*, 110–117. [CrossRef]

42. Suárez, L.; Castellano, J.; Romero, F.; Marrero, M.D.; Benítez, A.N.; Ortega, Z. Environmental Hazards of Giant Reed (*Arundo donax* L.) in the Macaronesia Region and Its Characterisation as a Potential Source for the Production of Natural Fibre Composites. *Polymer* **2021**, *13*, 2101. [CrossRef]

43. Prathap, K. A Comparative Study on the Mechanical Properties of Arundo Donax Epoxy Composites with Bamboo Epoxy Composites. *Int. J. Eng. Res. Technol.* **2019**, *8*, V8. [CrossRef]

44. Fiore, V.; Scalici, T.; Vitale, G.; Valenza, A. Static and Dynamic Mechanical Properties of Arundo Donax Fillers-Epoxy Composites. *Mater. Des.* **2014**, *57*, 456–464. [CrossRef]

45. Scalici, T.; Fiore, V.; Valenza, A. Effect of Plasma Treatment on the Properties of Arundo Donax L. Leaf Fibres and Its Bio-Based Epoxy Composites: A Preliminary Study. *Compos. B Eng.* **2016**, *94*, 167–175. [CrossRef]

46. Malnati, P. New Era for Rotomolding? Innovative Technology and Equipment Offer Superior Process Control and Produce Better Parts with Higher Repeatability and Reproducibility. *Plast. Eng.* **2019**, *75*, 10–13.

47. Suárez, L.; Barczewski, M.; Kosmela, P.; Marrero, M.D.; Ortega, Z. Giant Reed (*Arundo donax* L.) Fiber Extraction and Characterization for Its Use in Polymer Composites. *J. Nat. Fibers* **2023**, *20*, 2131687. [CrossRef]

48. Kubát, J.; Rigdahl, M.; Welander, M. Characterization of Interfacial Interactions in High Density Polyethylene Filled with Glass Spheres Using Dynamic-Mechanical Analysis. *J. Appl. Polym. Sci.* **1990**, *39*, 1527–1539. [CrossRef]

49. Jyoti, J.; Singh, B.P.; Arya, A.K.; Dhakate, S.R. Dynamic Mechanical Properties of Multiwall Carbon Nanotube Reinforced ABS Composites and Their Correlation with Entanglement Density, Adhesion, Reinforcement and C Factor. *RSC Adv.* **2016**, *6*, 3997–4006. [CrossRef]

50. Panwar, V.; Pal, K. An Optimal Reduction Technique for RGO/ABS Composites Having High-End Dynamic Properties Based on Cole-Cole Plot, Degree of Entanglement and C-Factor. *Compos. B Eng.* **2017**, *114*, 46–57. [CrossRef]

51. Mysiukiewicz, O.; Kosmela, P.; Barczewski, M.; Hejna, A. Mechanical, Thermal and Rheological Properties of Polyethylene-Based Composites Filled with Micrometric Aluminum Powder. *Materials* **2020**, *13*, 1242. [CrossRef]

52. Stanciu, M.D.; Teodorescu Draghicescu, H.; Tamas, F.; Terciu, O.M. Mechanical and Rheological Behaviour of Composites Reinforced with Natural Fibres. *Polymer* **2020**, *12*, 1402. [CrossRef]

53. Correa-Aguirre, J.P.; Luna-Vera, F.; Caicedo, C.; Vera-Mondragón, B.; Hidalgo-Salazar, M.A. The Effects of Reprocessing and Fiber Treatments on the Properties of Polypropylene-Sugarcane Bagasse Biocomposites. *Polymer* **2020**, *12*, 1440. [CrossRef]

54. Mohanty, S.; Nayak, S.K. Short Bamboo Fiber-Reinforced HDPE Composites: Influence of Fiber Content and Modification on Strength of the Composite. *J. Reinf. Plast. Compos.* **2010**, *29*, 2199–2210. [CrossRef]